Engineered Science
DOI: https://dx.doi.org/10.30919/es932

Adaptive Resource Allocation Scheme for Cooperative Transmission in Hybrid Simultaneous Wireless Information and Power Transfer for Wireless Powered Sensor Networks

N. Guler[1,*] and M. Salamah[2]

Abstract

This paper adopts the Simultaneous Wireless Information and Power Transfer (SWIPT) concept in designing an adaptive optimal resource allocation algorithm for cooperative transmission in hybrid SWIPT-enabled wireless power sensor networks. The SWIPT concept enables the sensor nodes to utilize the radio-frequency signals to transmit energy along with their sensed data to the cluster heads. We consider having a hybrid access point (HAP) that acts as both power transmitter and a communication gateway. Hence, a cluster head that is two-hops away from the HAP sends its aggregated data along with its harvested energy to its neighboring cluster head that is one-hop away from the HAP. The presented Adaptive Resource allocation scheme (ARCH) for Cooperative transmission in Hybrid simultaneous wireless information and power transfer for wireless powered sensor networks algorithm is an energy efficient iterative scheme proposed for energy efficiency optimization for cooperative transmission in a hybrid SWIPT-enabled wireless powered sensor network. For the intra-cluster and inter-cluster communication, sensor nodes adaptively choose time switching or power splitting mode based on their energy dispersed value. Also, we present a frame structure for enabling the hybrid SWIPT operation and we formulate the optimization problem by jointly optimizing the transmit powers, the SWIPT ratios, achievable rates, and time for transmission. Simulation results show that the proposed ARCH algorithm is superior to benchmark schemes in terms of energy efficiency, achievable rate, and dispersed energy.

Keywords: Simultaneous wireless information and power transfer (SWIPT); Energy efficiency; Radio frequency; Harvest energy; dispersed energy.
Received: 06 April 2023; Revised: 27 July 2023; Accepted: 28 July 2023.
Article type: Research article.

1. Introduction

One of the main challenges in wireless sensor networks (WSNs) is the battery constraint of the sensor nodes. Since WSNs typically consist of large number of sensor nodes, it is costly and inefficient to replace the sensor nodes' batteries regularly. It is also very common that sensing errors and link failures often occur when the battery life of a sensor node is almost expired. Therefore, a major challenge in WSN is improving the network lifetime and maximizing its performance.[1] WSNs are used for different purposes such as IoT, Robot Operating System (ROS),[2] monitoring purposes,[3] routing protocol enhancement,[4] and many more.

In WSNs, energy harvesting (EH) enables the sensor nodes to harvest energy from various environmental resources like solar, thermoelectricity, and wind. In literature, different works[5,6] adopted the concept of EH in WSNs aiming to extend the network lifetime. Authors in Ref. [7] adopted the EH concept that enables the sensor nodes to harvest energy from solar. The simulations show that their proposed scheme can effectively extend the lifetime of WSNs. Authors in Ref. [8], proposed an optimized wind-based EH system to sustain the operation of sensor nodes. However, these ambient energy sources are unstable, and cannot provide sustainable energy supply.

Unlike the EH, wireless power transfer (WPT) is another

[1] *Department of Informatics Engineering, University of Technology Bahrain, 1213 Block 712 Bldg. 829, Salmabad, Kingdom of Bahrain.*
[2] *Department of Computer Engineering, Eastern Mediterranean University, 99628, Famagusta, North Cyprus via Mersin 10, Turkey.*
**Email:* n.guler@utb.edu.bh (N. Guler)

new approach which provides more stable and reliable energy supply to sensor nodes by using radio-frequency (RF) signals.[9-11] Simultaneous Wireless Information and Power Transfer (SWIPT) is one of the energy harvesting mechanism based on radio frequency (RF) in which the receiver captures the ambient RF radiation and converts it into a direct current voltage through rectennas circuits.[12-14] With the SWIPT concept, the same RF received signal supports energy harvesting and information decoding at the same time by using a specific information energy splitting mechanism. In comparison with other energy sources, such as solar energy and wind energy, the desired RF is more reliable. Hence, SWIPT provides a new alternative for energy-constrained wireless devices to harvest energy and prolong the network lifetime. SWIPT is valuable in the future development of wireless sensor networks in harsh environments. Authors in Ref. [15], proposed a WPT-based power allocation and optimization strategy, in which the wireless sensor nodes are charged through receiving RF signals. Time switching (TS) and power splitting (PS) are the two energy information mechanisms used to employ SWIPT in practical systems. In TS mode, the receiver performs information decoding and energy harvesting in different time slots. Whereas, in PS mode, the power splitter divides the received power into two parts, one part for information decoding and the other for energy harvesting. It is envisioned that SWIPT can significantly improve the energy efficiency of the WSNs.[16] The hybrid access point (HAP) allows wireless information transfer (WIT) and the wireless power transfer (WPT) simultaneously. In this context, each sensor node harvests energy from the HAP and uses this energy for sensing, processing, and sending the data back to the HAP. The sensor nodes are usually randomly deployed for specific purposes and these nodes harvest energy differently from the HAP since the distance between the HAP and sensor node is different from the others. The node that is close to the HAP harvests more energy than the node that is deployed far away; in this case, there exists an energy efficiency gap. In this work, a detailed energy efficiency optimization problem is discussed.

In cluster-based WSNs, sensor nodes are grouped into several clusters where in each cluster one node is selected as the cluster head (CH). The sensor nodes send their sensed data to the CH which in turn aggregates the collected data as well as its own sensed data to send it to the HAP. As clustering the network has positive impact on reducing the total transmission cost in WSNs, in this paper, we present an adaptive optimal resource allocation algorithm for cooperative transmission in hybrid SWIPT-enabled cluster-based wireless power sensor networks.

In our work, we adopt the WPT technology in a WSN that uses a controllable RF power source, such as a power beacon and HAP. Hence, we consider the presence of the HAP which acts as both power transmitter and a communication gateway.[17] The network is referred as Wireless Powered Sensor Network (WPSN) with a hierarchical structure where the sensor nodes in each cluster send their sensed data to the CH. The CH in each cluster sends the aggregated data to the HAP if it is one-hop away or to the nearest neighbor CH if it is two-hops away. In our model, HAP transmits power beacons periodically to every sensor node which uses this harvested energy for sensing and sending the data to its CH. So the allocation of the network resources such as the power, power splitting ratio, time switching ratio, achievable rate, *etc*. can be optimized to maximize the network energy efficiency which is an important issue in WSNs. It is well known that if all sensor nodes perform the same task and thus generate equal sized sensed data, the maximum rate of the sensed data collected in a WSN will be limited by the worst sensor node with low harvesting energy and poor link budget.[18,19] Thus, all other sensor nodes need to support the same data rate as the worst node so that some sensor nodes may have energy remaining after transmitting their sensed data to the CH. On the other hand, the CH needs to do more processing for the reception and aggregation of multiple sensed data and has to transmit the aggregated data to the HAP. Thus, it requires more energy in general (*i.e*., the CH becomes the highest energy consuming node in the cluster). Considering this situation, we apply the SWIPT technique to the WPSN so that the sensor nodes can transfer their remaining energy to the CH while transmitting data on the same RF band. This approach can increase the sensed data rate in the cluster which boosts the network performance. The main objective of our study is to maximize the energy efficiency of the network while supporting the cooperative transmission in WPSN. To the author's best knowledge, this is the first work that considers hybrid SWIPT concept for optimizing the energy efficiency in a cooperative transmission of a cluster-based WPSN.

Our main contributions can be summarized as follows:

• We design a frame structure to operate hybrid SWIPT in the hierarchical WPSN configuration. The frame is divided into Wireless Power Transfer (WPT) and Wireless Information Transfer (WIT) slots, and each sensor node adaptively utilize the PS or TS mode in the allocated SWIPT slot based on the node's dispersed energy.

• We numerically express the achievable rate of sensed data in the system depending on the use of SWIPT.

• We develop an algorithm that finds the optimal SWIPT ratio in terms of PS and TS to maximize the energy efficiency for

cooperative transmission in WPSN.

• Finally, we propose a CH selection algorithm to maximize the energy efficiency of the network

The rest of this paper is organized as follows. In Section II, we survey related previous studies and point out the originality of our study. In Section III, we explain the network structure. Section IV presents the proposed ARCH algorithm and CH selection algorithm. In Section V, the simulation results are discussed. Finally, we present the conclusions in Section VI.

2. Literature survey

Recall that in SWIPT-enabled WPSNs, the sensor nodes can simultaneously perform energy harvesting and information decoding using the same received RF signal, which can improve the network performance. Different studies on SWIPT-enabled WPSNs have been presented in literature aiming at enhancing the network performance. For instance, energy efficiency optimization has been extensively studied in WPT communication systems.[15,20,21] Song and Zheng[11] studied resource assignment optimization problem to maximize energy efficiency in WPSNs with energy beamforming. Also, authors in Ref. [22] studied energy efficiency maximization problem by jointly optimizing harvesting time and transmit power with nonorthogonal multiple access (NOMA) based WPSNs.

Wang *et al*.[15] proposed a WPT-based power allocation optimization strategy, in which the wireless sensor nodes are charged through receiving RF signals. Huang *et al*.[23] studied the tradeoff between system energy efficiency and throughput to guarantee the minimum transmission rate. Tang *et al*.[24] studied the energy efficiency optimization for SWIPT-based MIMO two-way amplify-and-forward (AF) relaying networks through efficiently designing the PS ratio, in which the relay node forwards the source information by using the energy harvested from sources signals. Tang *et al*.[24] proposed a joint spatial switching and antenna selection scheme for QoS-constrained energy efficiency optimization in a MIMO SWIPT system.

SWIPT has also been applied to WSNs in various ways to overcome their energy limitations. Numerous surveys of SWIPT in WSNs have been published recently. For instance,[25] summarized the current research on SWIPT-based cooperative sensor networks, in which SWIPT is applied to WSNs in terms of dual-hop and multi-hop relays. Meanwhile, authors of Ref. [26] focused on the integral aspects of SWIPT in other prominent networks, such as device-to-device networks, vehicular ad hoc networks, wireless body area networks, WSNs, and so on. They presented open issues and challenges in SWIPT applications to such networks. In Ref. [27] an overview of SWIPT/WPT-enabled WSNs is provided where the network consists of multiple clusters and a sink node, in which the CH of each cluster performs SWIPT to give energy to relay nodes with low energies. In Ref. [28] a SWIPT-powered sensor network was considered in which each source node operates as both an information and energy transmitter, and the destination node works as an information receiver while the other nodes work as energy harvesters. Furthermore, authors in Ref. [29] and Ref. [30] applied the SWIPT concept in their routing algorithms aiming at enhancing the network lifetime. Energy efficiency optimization schemes have been presented in literature by exploiting the concept of SWIPT. In Ref [31] authors presented a smart agriculture based on SWIPT technology where energy efficiency optimization scheme is presented for green communication. In their scheme, the subcarriers' pairing and power allocation are jointly optimized using the Lagrangian dual function. Simulations showed that the proposed optimization scheme can efficiently improve the energy efficiency of the system. In Ref. [32] authors considered an orthogonal frequency division multiple access (OFDMA) system based on the SWIPT technology. Resource allocation algorithm was designed for maximizing the energy efficiency of data transmission to the receivers. In particular, the algorithm is based on power splitting hybrid receivers which are able to split the received signals into two power streams for concurrent information decoding and energy harvesting. Two scenarios are investigated considering different power splitting abilities of the receivers. In the first scenario, the receivers can split the received power into a continuous set of power streams with arbitrary power splitting ratios; whereas, in the second scenario, the receivers can split the received power into a discrete set of power streams with fixed power splitting ratios. By exploiting fractional programming and dual decomposition, suboptimal iterative resource allocation algorithms are developed to solve the nonconvex problems. Simulation results illustrate that their proposed scheme approached the optimal solution within a small number of iterations.

Most state-of-the-art schemes include SWIPT technique in EHWSNs focusing on maximizing the energy harvested that enhances the network throughout; however, such schemes didn't consider the wastage energy. In other words, in each cluster, the rate of transmission is limited to the minimum sensing rate of the nodes. Hence, sensor nodes do not need to use their whole harvested energy, but only portion of this energy to transfer minimum sensing rate and the rest of the energy is wasted. This motivated the proposed work study to take advantage of this extra energy of each node to send it to cluster head in intra-cluster communications as well as inter-

cluster communications. Also, it is worth noting that in previous studies the energy efficiency optimization in SWIPT system is studied based on PS or TS mode for intra-cluster communication. This has motivated the present work to include an adaptive selection of the SWIPT mode for cooperative transmission in a cluster-based WPSN, aiming at maximizing the energy efficiency.

3. Network structure

In this paper, we considered a cooperative cluster-based SWIPT-enabled wireless power sensor network, where the network consists of one hybrid access point (HAP) and k clusters, as shown in Fig. 1. The HAP is a power source that wirelessly transfers energy to sensor nodes and acts as a communication gateway. We assume CHs are either one-hop or two-hops away from the HAP. However, in each cluster, sensor nodes are considered to be one-hop away from the CH. Also, a CH uses cooperative transmission to send the aggregated data to the HAP only if it is two-hops away from the HAP. Therefore, in each cluster, the CH receives data from the cluster members and also might receive data from any neighboring CH that is two-hops away from the HAP.

The HAP periodically broadcasts an RF signal, and the nodes in each cluster harvest energy from this RF signal. The CH aggregates all of the sensing, and then sends the aggregated data along with its sensed data back to the HAP. In Fig. 1, we assume CH_1 is one-hop away from the HAP, and CH_2 is two-hops away from the HAP and therefore sends its aggregated data to the HAP by cooperating with CH_1.

We assume that sensor nodes adopt the harvest-then-transmit strategy.[33,34] Also, we assume that sensor nodes are hybrid SWIPT-enabled where each node either adopts the power splitting (PS) mode or the time switching (TS) mode[19] according to a specific condition which is explained in Section III. As shown in Fig. 2, each node contains a receiving antenna, a hybrid SWIPT unit (PS unit, TS unit), an energy harvester (EH) circuit, and an information encoder/decoder circuit. In the PS SWIPT mode, the node splits the received power into two ratios: ρ, is the power splitting ratio of the information decoding unit, and (1- ρ) is the power splitting ratio of the energy harvesting unit. In the TS SWIPT mode, the node splits the time into two ratios: β, is the time splitting ratio of the information encoding unit if it is a cluster member or information decoding unit if it is a cluster head, and (1-β) is the time splitting ratio of the energy harvesting unit. The antenna noise and the signal processing noise are denoted by n^A and n^S, respectively. The signal processing noise at the receiver side is modeled as Gaussian random variable with zero mean and variance σ^2. The harvested energy from a cluster member helps the cluster head to transmit with the targeted rate of transmission. We assume that sensors perform the same sensing task, such as temperature, humidity, or fire sensing, so that the bit size of the sensed data transmitted by each sensor node is the same. Each sensor node harvests different amount of energy depending on its distance from the HAP, and the power consumption needed for transmitting the data to the CH, as the distance between each sensor node and

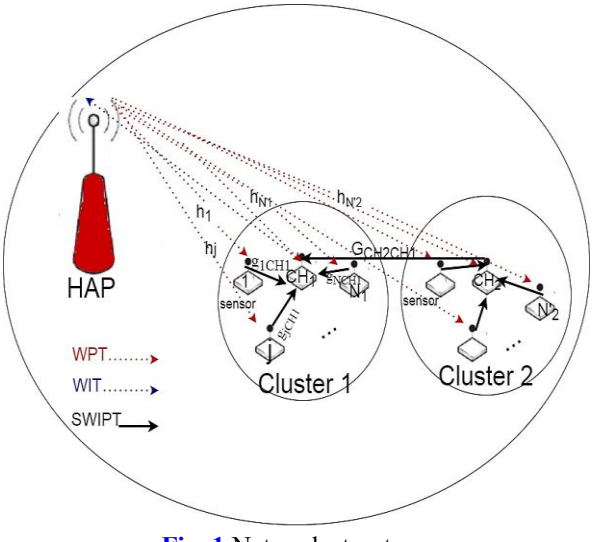

Fig. 1 Network structure.

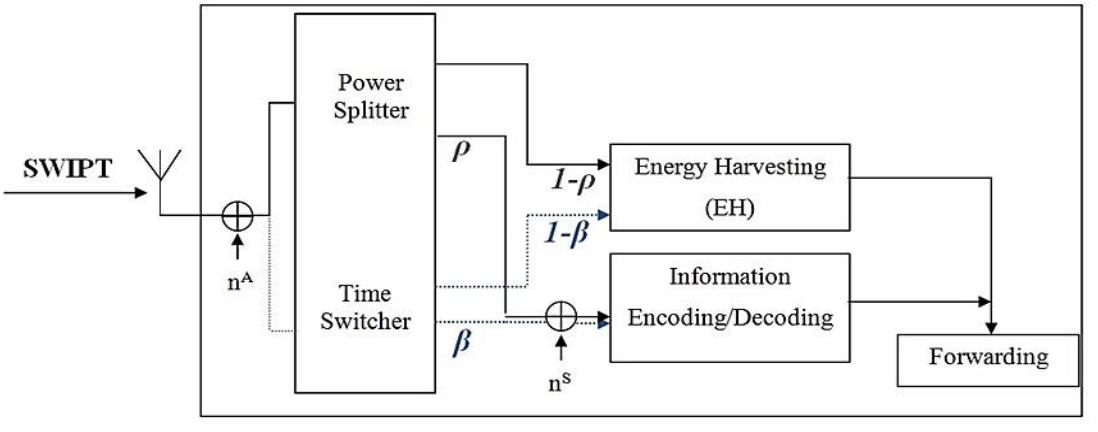

Fig. 2 A hybrid SWIPT-enabled node block diagram.

the CH varies. Hence, the maximum rate of the sensed data collection in a cluster is limited by the minimum rate of the transmission links. Therefore, in each cluster, sensor nodes do not need to consume the whole harvested energy. In fact, they only need to consume the energy required to support the maximum rate of sensed data and the remaining energy is unused. Since a CH usually requires extra energy for multiple receptions, processing, and transmission to the HAP, SWIPT-enabled sensor nodes transfer the remaining energy as well as their sensed data to the CH by applying the PS-SWIPT mode or the TS-SWIPT mode.

3.1 Frame structure

The proposed hybrid SWIPT frame structure is shown in Fig. 3 along with the detailed description of the adaptive resource allocation scheme for the cooperative transmission in hybrid SWIPT-enabled wireless-powered sensor networks is presented in this section. As it can be seen, the frame is based on time division multiple access with time division duplexing (TDMA/TDD) technology, and for the purpose of avoiding transmission conflict, scheduling-based resource allocation is adopted. At the beginning, the HAP broadcasts a beacon signal for frame synchronization and to provide the frame configuration and scheduling information to all of the nodes in the network. We assume the entire transmission duration of a frame is T seconds which is uniformly distributed among the clusters. In compliance with the harvest-then-transmit strategy,[34] the HAP transmits RF energy during the WPT slot with length T_e. We assume that we have two clusters (*i.e.* k =2): cluster1, which is one hop away from HAP, and cluster2 which is two-hop away from HAP. The sensor nodes in each cluster harvest energy during this WPT slot to use it in the current frame. The remainder of the frame is uniformly divided and used for each cluster. Hence, the allocated resources consist of three main hybrid SWIPT slots: one for intra-cluster communication of length δt (*i.e.* $\delta \times t$, where $2\delta < 1$) which is equally divided among the N_1 sensor nodes in cluster1 and N'_2 in cluster2; *i.e.*, each sensor node is allocated a time slot of length $\delta t/N_1$ in cluster1, and $\delta t/N'_2$ in cluster2. The second hybrid SWIPT slot is also of length δt, it is for the inter-cluster communication between CH_2 and CH_1. That is, the two-hop cluster head sends its collected data and remaining power to its one-hop cluster head during this second slot.[35] Note that during the first δt time slot, sensor nodes in cluster1 and cluster2 simultaneously harvest a ratio of power or time according to specific condition, then, send the sensed data to their cluster heads. In the second time slot, CH_2 uses the total harvested energy from the HAP and its sensor nodes to send its aggregated data to CH_1. The last time slot is the WIT slot; it is of length $(1-2\delta)t$, and used for transferring the collected data at CH_1 to the HAP. Each slot is reserved for each sensor node through a pre-scheduling mechanism so that access collision does not occur.[36] Each sensor node transmits the sensed data to its CH in the allocated SWIPT slot, and simultaneously transfers any remaining energy to the CH using either the PS-SWIPT or TS-SWIPT modes. The SWIPT concept is applied in each cluster whenever the sensing rate of the corresponding CH is less than the minimum sensing rate of cluster members. In such a case, for instance, when looking at cluster1 with the PS SWIPT mode, each sensor node i uses a portion ρ_i of power for WIT (*i.e.* information transfer to CH_1), and the remaining portion $(1-\rho_i)$ for WPT (*i.e.* transferring energy to CH_1). Whereas each sensor node j in cluster2 which is two-hop away from HAP uses α_j portion of power for information transfer to CH_2, and $(1-\alpha_j)$ portion for WPT. SWIPT concept is also applied for CH_2 when sending its aggregated data to CH_1. In this case, CH_2 uses υ portion of power for sending its aggregated data and $(1-\upsilon)$ portion for WPT. Similarly, in the case of applying the TS mode, each sensor node i uses a portion β_i of time for WIT, and the remaining portion $(1-\beta_i)$ for WPT. Moreover, each sensor node j in cluster2 uses ω_j portion of time for WIT, and $(1-\omega_j)$ portion for WPT. Moreover, CH_2 uses φ portion of time to send its aggregated data to CH_1 along with $(1-\varphi)$ portion for WPT. Finally, CH_1 aggregates all of the sensing information and transmits the aggregated sensed data to the sink in its allocated WIT slot. Note that, CH_1 uses not only the energy initially provided by the HAP but also the energy additionally received from its member nodes and neighboring CH_2. Applying the SWIPT concept, as described above, facilitates an efficient energy transfer as well as data transmission.

In our analysis, we assume that we have two clusters; cluster1 and cluster2. Cluster 1 is one-hop away from the HAP with N1 number of nodes; and cluster2 is two-hops away from the HAP with N2 number of nodes. As seen in Fig. 3, each sensor node harvests energy from HAP during the T_e WPT slot. In cluster1, the harvested energy of sensor node $i \neq CH_1$, is denoted by E_i^h and given by Eq. (1), where h_i is the channel power gain between the HAP and sensor node i; ζ_i is the energy harvesting efficiency ($0 < \zeta_i < 1$); and P is the power transmitted by the HAP during time slot T_e. The harvested energy in cluster2 is similarly determined as in cluster1, and given by Eq. (2).

$$E_i^h = h_i \zeta_i \, PT_e, \forall \, i \in N_1, i \neq CH_1 \quad (1)$$

$$E_j^h = h_j \zeta_j \, PT_e, \forall \, j \in N_2, j \neq CH_2 \quad (2)$$

The transmission power of sensor node j for transmitting data to CH_2 during its time slot $\delta t/N_2$ is given by Eq. (3):

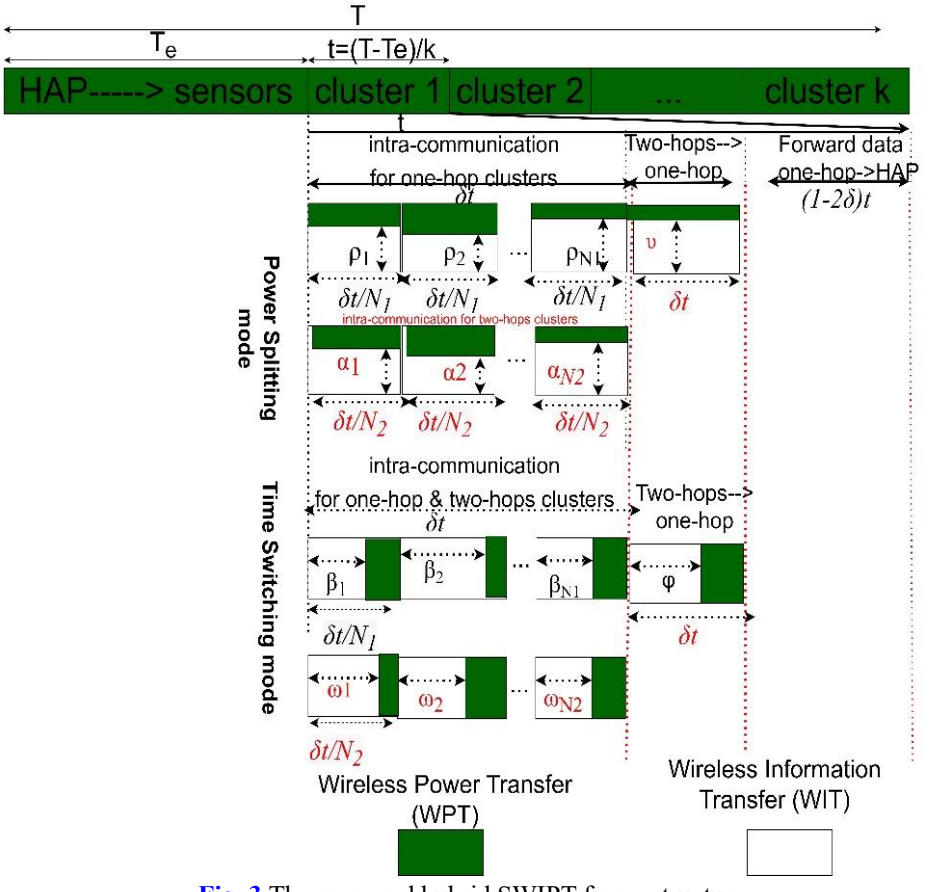

Fig. 3 The proposed hybrid SWIPT frame structure.

$$P_j=\frac{N_2\eta_j E_j^h}{\delta t}=\frac{N_2\eta_j\zeta_j h_j P T_e}{\delta t},\ \forall\ j\in N_2, j\neq CH_2 \quad (3)$$

where $0<\eta\_j<1$ is the energy harvest coefficient of node j.

According to Shannon's theorem, the achievable rate of transmission in cluster2 from sensor node j to the CH_2 is given by Eq. (4):

$$R_{j_{CH_2}}=\frac{\delta t}{N_2}\log_2\left(1+\frac{g'_{jCH_2}P_j}{\sigma^2}\right),\ \forall\ j\in N2, j\neq CH_2 \quad (4)$$

where g'jCH$_2$ is the channel power gain from sensor node j to CH2, and σ^2 is the noise power at the receiving side. Note that the unit of this rate has bits/Hz reflecting the transmission time $\frac{\delta t}{N_2}$.

Similarly, the achievable rate of transmission in cluster1 from sensor node i to the cluster head CH_1 is given by Eq. (5):

$$R_{i_{CH_1}}=\frac{\delta t}{N_1}\log_2\left(1+\frac{g_{iCH_1}P_i}{\sigma^2}\right),\ \forall\ i\in N1, i\neq CH_1 \quad (5)$$

Case A: No need to apply SWIPT technique.

In this case, the rate of transmission at a cluster head is greater than the minimum rate of transmission from its cluster members.

Case A.1: For inter-communication (CH_2 sending to CH_1): Then, CH_2 uses the harvest energy from HAP to send its aggregated data to its closest neighbor cluster head CH_1. Therefore, the transmission power of CH_2 at transmission time δt is given by Eq. (6):

$$P_{CH_2}=\frac{\eta_{CH_2}E^h_{CH_2}}{\delta t}=\frac{\eta_{CH_2}h_{CH_2}\zeta_{CH_2}PT_e}{\delta t} \quad (6)$$

And, the achievable rate for cooperative transmission from CH_2 to CH_1 is given by Eq. (7):

$$R_{CH_{2CH_1}}=\delta t\log_2\left(1+\frac{G_{CH_2CH_1}P_{CH_2}}{\sigma^2}\right) \quad (7)$$

Hence, the maximum rate of sensed data for inter-communication (cluster2→cluster1) is determined by Eq. (8):[37]

$$R^{Inter}_{no-swipt}=\min[R^{cluster2}_{no-swipt}, R^{cluster1}_{no-swipt}] \quad (8)$$

Case A.2: *For intra-communication inside cluster1:* In regards to cluster1, the transmission power of CH_1 for transmitting data during WIT slot to HAP is given by Eq. (9):

$$P_{CH_1}=\frac{\eta_{CH_1}E^h_{CH_1}}{(1-2\delta)t}=\frac{\eta_{CH_1}h_{CH_1}PT_e}{(1-2\delta)t} \quad (9)$$

And, the achievable rate of transmission from CH_1 to HAP during (1-2δ)t is given by Eq. (10):

$$R_{CH_1}=(1-2\delta)t\log_2\left(1+\frac{h_{CH_1}P_{CH_1}}{\sigma^2}\right) \quad (10)$$

Also, the maximum rate of sensed data for intra-communication in cluster1 is limited by the minimum rate of the transmission links[19,35,37] and given by Eq. (11):

$$R^{CH_1}_{no-swipt}=\min[\min_{i\in N_1, i\neq CH_1}\{R_{iCH_1}\},\ R_{CH_1}] \quad (11)$$

Case A.3: For intra-communication inside cluster2:

The maximum rate of sensed data that can be collected in cluster2 is also limited by the minimum rate of the transmission links.[19,35] Therefore, the achievable rate of sensed data in cluster2 is determined by Eq. (12):

$$R^{cluster2}_{no-swipt}=\min[\min_{j\in N2, j\neq CH2}\{R_{jCH2}\},\ R_{CH_2}] \quad (12)$$

Case B: There is a need for applying SWIPT technique.

$$S=\begin{cases} TS\ if \begin{cases} Pi-\frac{\sigma^2(2^{\frac{R_{no-swipt}^{Intra-cluster1}}{\frac{\delta t}{N_1}}}-1)}{g_{ia}}=0;\ \forall\ i\epsilon\ N_1, i\neq CH_1 OR\ R_{CH_1}<\min_i R_{iCH_1}\ \forall\ i\epsilon\ N_1, i\ i\neq CH_1 \\ Pj-\frac{\sigma^2(2^{\frac{R_{no-swipt}^{cluster2}}{\delta t/N2}}-1)}{g'_{jCH_2}}=0;\ \forall\ j\epsilon\ N_2, j\neq CH_2 OR\ R_{CH_2}<\min_j R_{jCH_2}, \forall\ j\ \epsilon\ N_2, j\neq CH_2 \\ P_{CH_1}-\frac{\sigma^2(2^{\frac{R_{no-swipt}^{Inter}}{(1-2\delta)t}}-1)}{h_{CH_1}}<P_{CH_2}-\frac{\sigma^2(2^{\frac{R_{no-swipt}^{Inter}}{\delta t}}-1)}{G_{CH_2CH_1}};\forall\ CH_1\neq CH_2 \end{cases} \\ PS\quad Otherwise \end{cases} \tag{13}$$

In this case, the rate of transmission at a cluster head is less than the minimum rate of transmission from its members. Hence, for a cluster head to be capable of transmitting the achieved rate, each cluster member will use either PS ratio or TS ratio of its energy harvesting and send this ratio energy along with its data to its cluster head. This is valid for all clusters. So, the SWIPT mode S is determined as in Eq. (13).

Therefore, S is either power splitting or time switching, based on the value of the dispersed power of a node, which is the power difference between the power needed to transmit the achievable rate and the harvested one. This work considers the harvest-then-transmit protocol to be used by sensor nodes, hence, a major challenge lies on the tradeoff between achievable throughput and energy harvesting opportunity of sensor nodes. Confronting this challenge, proposed scheme applies the TS mode when the difference between the achieved rate of the CH is less than the minimum achievable rate in the cluster for intra communication and when the achievable rate at the one-hop CH is less than achievable rate at the two-hop CH for inter-communication. Otherwise, PS mode is applied. When the SWIPT mode is used then its flag is 1 as in Eq. (14).

$$\text{Flag(S)}=\begin{cases} 1\ if\ S\ is\ used \\ 0\ \text{Otherwise} \end{cases} \tag{14}$$

CaseB.1: Power Splitting (PS) SWIPT mode:

As shown in Fig. 3 and starting with cluster1, each sensor node i uses ρ_i of the harvested power for data encoding in WIT slot and sends $(1-\rho_i)$ of the harvested power for energy harvesting CH_1 along with the encoded data in the WPT slot. Hence, the achievable rate of transmission in the cluster1 from sensor node i to CH_1 is given by Eq. (15):

$$R_{iCH_1}{}^{PS}=\frac{\delta t}{N_1}\log_2(1+\frac{g_{iCH_1}\rho_i P_i}{\sigma^2}),\ \forall\ i\epsilon\ N_1, i\neq CH_1 \tag{15}$$
$$=\frac{\delta t}{N_1}\log_2(1+\frac{\eta_i\zeta_i g_{iCH_1}\rho_i P\ h_i N_1 T_e}{\delta t\sigma^2})$$

Also, the achievable rate of transmission in the cluster 2 from sensor node j to CH_2 is given by Eq. (16):

$$R_{jCH_2}{}^{PS}=\frac{\delta t}{N_2}\log_2(1+\frac{g'_{jCH_2}\alpha_j P_j}{\sigma^2}),\ j\epsilon\ N_2, j\neq CH_2 \tag{16}$$
$$=\frac{\delta t}{N_2}\log_2(1+\frac{\zeta_j\eta_j g'_{jCH_2}\alpha_j P\ h_j N'_2 T_e}{\delta t\sigma^2})$$

Also, the extra energy obtained at CH_2 from its cluster members is given by Eq. (17):

$$E_{CH_2}{}^{PS\_extra}=\sum_{j=1}^{(N_2-1)}\zeta_j P_j g'_{jCH_2(1-\alpha_j)}\frac{\delta t}{N_2} \tag{17}$$

And, the achievable rate for cooperative transmission from CH_2 to CH_1 is given by Eq. (18) and from CH_1 to HAP is given by Eq. (19):

$$R_{CH_2CH_1}{}^{PS}=\delta t\log_2(1+\frac{G_{CH_2CH_1}vP_{CH_2}{}^{PS}}{\sigma^2}) \tag{18}$$

$$R_{CH_1}{}^{PS}=(1-2\delta)t\log_2(1+\frac{P_{CH_1}{}^{PS}h_{CH_1}}{\sigma^2}) \tag{19}$$

And, the extra energy obtained at CH_1 from cluster members and CH_2 is given by Eq. (20):

$$E_{CH_1}{}^{PS\_extra}=\sum_{i=1}^{(N_1-1)}\zeta_i P_i g_{iCH_1(1-\rho_i)}\frac{\delta t}{N_1}+\delta t(1-\upsilon)\ E_{CH_2}{}^{extra} \tag{20}$$

Hence, the transmission power at CH_2 is given by Eq. (21):

$$P_{CH_2}{}^{PS}=\frac{\eta_{CH_2}(E_{CH_2}^{h}+E_{CH_2}{}^{PS\_extra})}{\delta t} \tag{21}$$

And, the transmission power at CH_1 is given by Eq. (22):

$$P_{CH_1}{}^{PS}=\frac{\eta_{CH_1}(E_{CH_1}^{h}+E_{CH_1}{}^{PS\_extra})}{(1-2\delta)t} \tag{22}$$

CaseB.2: Time Switching (TS) SWIPT:

Each sensor node i uses β_i of the time slot t, as shown in Fig. 3, for data encoding in WIT slot and uses the remaining time $(1-\beta_i)$ t for WPT. Hence, the achievable rate of transmission in the cluster1 is given by Eq. (23):

$$R_{iCH_1}{}^{TS}=\frac{\beta_i\delta t}{N_1}\log_2(1+\frac{g_{iCH_1}P_i}{\sigma^2}),\ \forall\ i\epsilon\ N_1, i\neq CH_1 \tag{23}$$
$$=\frac{\beta_i\delta t}{N_1}\log_2(1+\frac{\zeta_i\eta_i g_{iCH_1}P\ h_i N_1 T_e}{\delta t\sigma^2})$$

In cluster2, each sensor node j uses ω_j t time slot, as shown in Fig. 3, for data encoding in WIT slot and uses the remaining time $(1-\omega_j)$ t for WPT. Hence, the achievable rate of transmission in the cluster2 from sensor node j to CH_2 is given by Eq. (24):

$$R_{jCH_2}{}^{TS}=\frac{\omega_j\delta t}{N_2}\log_2(1+\frac{g'_{jCH_2}P_j}{\sigma^2}),\ \forall\ j\epsilon\ N_2, j\neq CH_2 \tag{24}$$
$$=\frac{\omega_j\delta t}{N_2}\log_2(1+\frac{\eta_j\zeta_j g'_{jCH_2}P\ h_j N'_2 T_e}{\delta t\sigma^2})$$

and the achievable rate for cooperative transmission from the CH_2 to CH_1 is given by Eq. (25) and from CH_1 to HAP is given by Eq. (26):

$$R_{CH_2CH_1}{}^{TS}=\varphi\delta t\log_2(1+\frac{G_{CH_2CH_1}P_{CH_2}{}^{TS}}{\sigma^2}) \tag{25}$$

$$R_{CH_1}{}^{TS}=(1-2\delta)t\log_2(1+\frac{P_{CH_1}{}^{TS}h_{CH_1}}{\sigma^2}) \tag{26}$$

Also, the extra energy obtained at CH_2 from its cluster members is given by Eq. (27):

$$E_{CH_2}{}^{TS\_extra}=\sum_{j=1}^{(N_2-1)}\zeta_j P_j g'_{jCH_2}\frac{(1-\omega_j)\delta t}{N_2} \tag{27}$$

Similarly, the extra energy obtained at CH_1 from its cluster members and CH_2 is given by Eq. (28):

$$E_{CH_1}{}^{TS\_extra}=\sum_{i=1}^{(N_1-1)}\zeta_i P_i g_{iCH_1}\frac{(1-\beta_i)\delta t}{N_1}+E_{CH_2}{}^{TS\_extra}$$

$$= \sum_{i=1}^{(N_1-1)} \zeta_i P_i g_{iCH_1} \frac{(1-\beta_i)\delta t}{N_1} + (\sum_{j=1}^{(N_2-1)} \zeta_j P_j g'_{jCH_2} \frac{(1-\omega_j)\delta t}{N_2}) \quad (1\text{-}\upsilon)\ \delta t \quad (28)$$

Hence, the transmission power at CH_2 is given by Eq. (29):

$$P_{CH_2}{}^{TS} = \frac{\eta_{CH_2}(E^h_{CH_2} + E_{CH_2}{}^{TS\_extra})}{\delta t} \quad (29)$$

And, the transmission power at CH_1 is given by Eq. (30):

$$P_{CH_1}{}^{TS} = \frac{\eta_{CH_1}(E^h_{CH_1} + E_{CH_1}{}^{TS\_extra})}{(1-2\delta)t} \quad (30)$$

Now, since the maximum rate of sensed data that can be collected in cluster2 is also limited by the minimum rate of the transmission links; therefore, the achievable rate of sensed data in cluster2 under S which is given by Eq. (31):

$$R_S^{cluster2} = \min[\min_{j\in N_2, j\neq CH_2}\{R_{jCH_2}{}^S\},\ R_{CH_2}{}^S]$$

$$= \begin{cases} \min\left(\min\left(\frac{\omega_j \delta t}{N_2}\log_2(1+\frac{g'_{jCH_2}P_j}{\sigma^2}\right), \forall j\in N_2, j\neq CH_2\right), \varphi\delta t\log_2(1+\frac{G_{CH_2CH_1}P_{CH_2}{}^{TS}}{\sigma^2})); \ if\ TS\ mode \\ \min(\min(\frac{\delta t}{N_2}\log_2(1+\frac{g'_{jCH_2\alpha_j}P_j}{\sigma^2}), \forall j\in N_2, j\neq CH_2), \delta t\log_2(1+\frac{G_{CH_2CH_1\upsilon P_{CH_2}{}^{PS}}}{\sigma^2}) ;\ \text{if PS mode} \end{cases} \quad (31)$$

Similarly, the maximum rate of sensed data for intra-communication in cluster1 is determined by Eq. (32):

$$R_S^{cluster1} = \min[\min_{i\in N_1, i\neq CH_1}\{R_{iCH_1}{}^S\},\ R_{CH_1}{}^S]$$

$$= \begin{cases} \min\left(\min\left(\frac{\beta_i \delta t}{N_1}\log_2(1+\frac{g_{iCH_1}P_i}{\sigma^2}\right), \forall i\in N_1, i\neq CH_1\right), (1-2\delta)t\log_2(1+\frac{P_{CH_1}{}^{TS}h_{CH_1}}{\sigma^2})); \ if\ TS\ mode \\ \min\left(\min\left(\frac{\delta t}{N_1}\log_2(1+\frac{g_{iCH_1}\rho_i P_i}{\sigma^2}\right), \forall i\in N_1, i\neq CH_1\right), (1-2\delta)t\log_2(1+\frac{P_{CH_1}{}^{PS}h_{CH_1}}{\sigma^2}) ;\ \text{if PS mode} \end{cases} \quad (32)$$

If $ts = (1-2\delta)/\delta$; then $R_S^{cluster1}$ is rewritten as shown in Eq. (33):

$$= \begin{cases} \min(\min(\frac{\beta_i}{N_1}\log_2(1+\frac{g_{iCH_1}P_i}{\sigma^2}), \forall\ i\in N_1, i\neq CH_1), ts\log_2(1+\frac{P_{CH_1}{}^{TS}h_{CH_1}}{\sigma^2})); \ if\ TS\ mode \\ \min(\min(\frac{1}{N_1}\log_2(1+\frac{g_{iCH_1}\rho_i P_i}{\sigma^2}), \forall i\in N_1, i\neq CH_1), ts\log_2(1+\frac{P_{CH_1}{}^{PS}h_{CH_1}}{\sigma^2}) ;\ \text{if PS mode} \end{cases} \quad (33)$$

Hence, the Total system achievable is determined by Eq. (34):

$$R_{...S}^{Inter} = R_S^{cluster1} + R_S^{cluster2} \quad (34)$$

The energy dissipated CH_2 is given by Eq. (35) and that of sensor node j in cluster2 is given by Eq. (36):

$$Edisp^{CH_2} = P_{CH_2}{}^S - \frac{\sigma^2}{G_{CH_2CH_1}}(2^{\frac{R_S^{cluster2}}{\delta t}} - 1) \quad (35)$$

$$Edisp^j = \begin{cases} 0\ ;\ if\ R_{CH_2} < \min_j R_{jCH2}\ \forall j\in N_2, j\neq CH_2 \\ P_j - \frac{\sigma^2}{g'_{jCH_2}}(2^{\frac{R_{no-swipt}^{cluster2}}{\frac{\delta t}{N_2}}}); otherwise \end{cases} \quad (36)$$

The energy dissipated of cluster2 is given by Eq. (37).

$$Edisp^{cluster2} = Edisp^{CH_2} + \sum_{\forall j\in N_2, j\neq CH_2} Edisp^j \quad (37)$$

The energy dissipated in cluster1 is calculated in the same way as in Eq. (37); the energy dissipated in the system is the sum of energy dissipated of each cluster in the system.

4. The proposed ARCH algorithm

4.1 Problem formulation

Resource allocation optimization for the cooperative transmission in the hybrid SWIPT-enabled Wireless Power Transfer Sensor Network incorporates different energy harvesting parameters that are difficult to solve due to the non-linearity form of the energy harvester model. Hence, the optimization problem becomes non-convex. Therefore, we try to convert the optimization problem to convex so that we can apply the Dinkelbach method[38] in our proposed iterative algorithm to solve the optimization problem. For simplicity, we assume the SWIPT ratios of cluster members in all clusters are of same value; specifically ρ,α are the same ,and β,ω are the same.

The total transmission throughput in the system is given by Eq. (38):

$$R_{(P_A,P_B,\ \rho,\beta,\upsilon,\omega,\varphi,\alpha,\delta)} = R_S^{Inter} \quad (38)$$

where S is given by Eq. (13).

The total consumption power is given by Eq. (39):

$$\Upsilon_{(P_A,P_B,\ \rho,\beta,\upsilon,\omega,\varphi,\alpha,\delta),\forall i\in N\setminus\{a\},\forall j\in N\setminus\{b\}} = (N_1\times P_i/\zeta_i + N_2\times P_j/\zeta_j + P_{CH_2}/\zeta_{CH_2} + P_{CH_1}/\zeta_{CH_1} + P_{ctx} + (1-2\delta)tP_{ctx} \quad (39)$$

where ζ denotes the power amplifier efficiency, P_{ctx} is the circuit power consumption at nodes as transmitters, P_{crx} is the constant circuit power consumed at the cluster heads CH_1 and CH_2 as receivers. The system energy efficiency (EE) denoted by Ƒ and given in Eq. (40), is defined as the ratio of the system throughput in bits to the system power consumption in joules.

$$Ƒ_{(P^S{}_1,P^S{}_2,\ \rho,\beta,\upsilon,\omega,\varphi,\alpha,\delta)} = \frac{R_{(P^S{}_1,P^S{}_2\ \rho,\beta,\upsilon,\omega,\varphi,\alpha,\delta)}}{\Upsilon_{(P^S{}_1,P^S{}_2\ \rho,\beta,\upsilon,\omega,\varphi,\alpha,\delta)}} \quad (40)$$

where S can be either power splitting or time switching and P^S is given in (13). In order to find the maximum energy harvesting in the system, we set the maximum energy efficiency cost as the optimization problem which is formulated as OPT1 in Eq. (41). The optimization variables are the power policy $\mathbf{p}=\{P^S{}_t \geq 0,\ t\epsilon\{N_1\cup N_2\}$, the SWIPT splitting policy of nodes in cluster1, nodes in cluster2, and cluster head CH_2, $\mathbf{ş}=\{\rho_i,\beta_i\ i\epsilon N_1\ ,\alpha_j,\omega_j, j\epsilon N_2, \upsilon, \varphi\}$, and time proportion **δ**.

OPT1:

$$\max_{(p,ş,\delta)} Ƒ_{(p,ş,\delta)} \quad (41)$$

s.t. C1: $R_S{}^2 \geq R_{min}$;C2: $R_S{}^1 \geq R_{min}$; C3: $0 < P^S{}_t \leq P_{max}$, $t\epsilon$

$\{N_1 \cup N_2\}$;
C4: $E_t^h \geq 0$, tϵ $\{N_1 \cup N_2\}$; C5: $0 < \delta < 0.5$;C6: $0 < \rho_{i,} < 1$, iϵN_1,i$\neq CH_1$;
C7: $0 < \alpha_j < 1$, jϵ N_2,j$\neq CH_2$; C8: $0 < \upsilon < 1$;C9: $0 < \varphi < 1$;C10: $0 < \beta_{i,} < 1$; iϵN_1,i$\neq CH_1$; C11: $0 < \omega_j < 1$, jϵ N_2,j$\neq CH_2$; where C1 and C2 are the data transmission rate constraint under either PS or TS mode that require the achievable rate should be above R_{min}, C3 indicates that the transmission power of any node should be bounded by maximum transmission power denoted by P_{max} is, C4 is the harvested energy constraint. C5 is the time ratio constraint. C6 indicates that the SWIPT splitting ratio is bounded for cluster1 and same for cluster2 in C7 – C11. We assume ζ has same value for all sensor nodes. Since some of the existing constraints are non-convex and coupling relationships exist among different optimization variables and the non-convex constraints; then, the optimization problem is non-convex. Therefore, to deal with this coupling relationship, we let ts = $\frac{(1-2\delta)}{\delta}$, so OPT1 can be rewritten as shown in Eq. (42):

OPT2:

$$\max_{(\mathcal{P},\rho,t)} R'^{S}_{CH_2} + R'^{S}_{CH_1} - q^*(N_1 \times P^{S}_{i}/\zeta + N_2 \times P^{S}_{j}/\zeta + P^{S}_{CH_2}/\zeta + P^{S}_{CH_1}/\zeta + P_{ctx} + tsP_{crx})$$
$$= R'^{*S}_{CH_2} + R'^{*S}_{CH_1} - q^*(N_1 \times P^{S}_{i}{}^{*}/\zeta + N_2 \times P^{S}_{j}{}^{*}/\zeta + P^{S}_{CH_2}{}^{*}/\zeta + P^{S}_{CH_1}{}^{*}/\zeta + P_{ctx} + ts^*P_{crx}) = 0 \quad (46)$$

Proof:
Based on Eq. (17-39), $\mathcal{F}_{(P^{S}_1, P^{S}_2, \rho,\beta,\upsilon,\omega,\varphi,\alpha,\delta)}$ given by Eq. (40) is positive. Moreover, Đ(Ƥ, ρ, t) and q* are defined in Eq. (44, 45); so the rest of the proof can be continued by following similar method as in Ref. [39] Thus the problem in OPT2 can be transformed by solving the parametric problem of OPT3 as in Eq. (47).

OPT3:

$$\max_{(\mathcal{P},ş,ts)} R'^{S}_{CH_2} + R'^{S}_{CH_1} - q\,(N_1 \times P^{S}_{i}/\zeta + N_2 \times P^{S}_{j}/\zeta + P^{S}_{CH_2}/\zeta + P^{S}_{CH_1}/\zeta + P_{ctx} + tsP_{crx}) \quad (47)$$

s.t. C1-1, C2-1, C3, C4, C5-1, C6-C11, q is a given parameter. Still OPT3 is non-convex due to coupling between Ƥ, ş and the non-convex constraints; therefore, we introduce the following variables into the problem:

$r_{CH_1} = R'^{S}_{CH_1}$, $r_{CH_2} = R'^{S}_{CH_2}$, $xi = \begin{cases} (1-\rho_i)P_{i \text{ if S=PS in eq.(13)}} \\ P_{i \text{ if S=TS in eq.(13)}} \end{cases}$;

$i\epsilon N_1$, $xj = \begin{cases} (1-\alpha_j)P_{j \text{ if S=PS in eq.(13)}}; j\epsilon N_2 \\ P_{j \text{ if S=TS in eq.(13)}} \end{cases}$,

$xb = \begin{cases} (1-v)P_{b \text{ if S=PS in eq.(13)}} \\ P_{b \text{ if S=TS in eq.(12)}} \end{cases}$

Then, the optimization problem OPT3 can be equivalent to OPT4 as in Eq. (48):

OPT4:

$$\max_{(\mathcal{P},ş,x_i,x_j,r_{CH_1},r_{CH_2},t)} r_{CH_1} r_{CH_2} q(N_1 \times P^{S}_{i}/\zeta + N_2 \times P^{S}_{j}/\zeta + P^{S}_{CH_2}/\zeta + P^{S}_{CH_1}/\zeta + P_{ctx} + tsP_{crx}) \quad (48)$$

s.t. C1-2: $r_{CH_1} \geq R_{min}$ (t+2);C2-2: $r_{CH_2} \geq R_{min}$(t+2);C3-1: $0 < x_i, x_j, x_{CH_2} < P_{max}$; i ϵ N_1, $j \epsilon N_2$; C4, C5-1,C6-C11;C12: $tsB \log_2\left(1 + \frac{(Pixi)|h_a|^2}{W\sigma 2}\right) \geq r_{CH_1}$, i$\epsilon$ N_1 ;C13: $Blog_2\left(1 + \frac{(Pjxj)|h_j|^2}{W\sigma 2}\right) \geq r_{CH_2}$, j$\epsilon$ N_2

The optimization of OPT4 is convex. Proof in the Appendix. Solving the optimization of OPT1 is carried using the proposed ARCH algorithm presented in the next section and which is based on Dinkelbach method.

4.2 ARCH algorithm

$$\max_{(p,ş,\frac{1}{ts+2})\forall\, i\epsilon N_1, j\epsilon N_2} \frac{R'^{S^2} + R'^{S^1}}{(N_1 \times P^{S}_{i}/\zeta + N_2 \times P^{S}_{j}/\zeta + P^{S}_{b}/\zeta + P^{S}_{a}/\zeta + P_{ctx}) + tsP_{crx}} \quad (42)$$

s.t. C1-1: $R'^{2}_{S} \geq R_{min}$ (ts+2); C2-1: $R'^{1}_{S} \geq R_{min}$(ts+2); C5-1: ts > 0; C3, C4, C6-C11; Let (Ƥ*, ş*, ts*) be the optimal solution to OPT2, so the optimal solution to OPT1 is given by (Ƥ*, ş*, δ*), where $\delta^* = 1/(ts^* + 2)$. In order to solve OPT1, we apply Dinkelbach method[38] to convert the fraction form of the optimization problem into an equivalent subtractive form as given by Eq. (43):

$$Đ(\mathcal{P}, ş, ts) = Ŗ^{(\mathcal{P},ş,ts)} - q^* Ţ^{(\mathcal{P},ş,ts)} \quad (43)$$

where q* is the maximum EE for the cooperative transmission given by Eq. (44) and q is given by Eq. (45):

$$q^* = \frac{Ŗ^{(\mathcal{P}^*, ş^*, ts^*)}}{Ţ^{(\mathcal{P}^*, ş^*, ts^*)}} = \max_{(\mathcal{P},ş,ts)} q(\mathcal{P}, ş, ts) \quad (44)$$

s.t. C1-1: $R'^{2}_{S} \geq R_{min}$ (ts+2); C2-1: $R'^{1}_{S} \geq R_{min}$(ts+2);C5-1: 0 < t; C3, C4, C6-C11; where

$$q = \frac{R'^{S^2} + R'^{S^1}}{(N_1 \times P^{S}_{i}/\zeta + N_2 \times P^{S}_{j}/\zeta + P^{S}_{b}/\zeta + P^{S}_{a}/\zeta + P_{ctx}) + tsP_{crx}} \quad (45)$$

Lemma 1: The maximum value of EE q* is achieved iff Eq. (43) is satisfied and given by Eq. (46)

We have presented an iterative algorithm which is based on Dinkelbach method to solve the OPT1, as shown in Table 1. We have used the CVX method[40] with a given value of energy efficiency q to solve the optimization problem OPT4, and to determine the optimal solutions denoted by $(P_1', P_2', x_i', x_j', r_{CH_1}', r_{CH_2}', ts')$. With a given error maximum bound œ, the optimal solutions to OPT1 can be obtained when

$$r_{CH_1}' + r_{CH_2}' - (N_1 \times P^{S'}_{i}/\zeta + N_2 \times P^{S'}_{j}/\zeta + P^{S'}_{CH_2}/\zeta + P^{S'}_{CH_1}/\zeta + P_{ctx} + ts'P_{crx}) < œ$$

is satisfied. Assume that the interior point method is used to obtain optimal solution to OPT4 with maximum number of

Table 1. ARCH Algorithm.

Input: I_{max}: maximum iteration, œ: maximum error
Output: $\mathcal{P}^*, \S^*$: optimal resource allocation policy Optimal energy efficiency q*, optimal throughput $\mathcal{R}^*$, optimal power consumption $\mathcal{T}^*$, optimal time slot portion δ^*
q←0; iteration index: I=0, Flag=0;
repeat
Solve OPT4 with the given q by using the CVX method[40] and obtain the optimal solution ($P_i', P_j', x_i', x_j', r_{CH_1}', r_{CH_2}', ts'$) and $\mathcal{D}(\mathcal{P}', \S', ts')$
If $\mathcal{D}(\mathcal{P}', \S', ts') <$ œ then
Set $P_i^* \leftarrow P_i'$, $P_j^* \leftarrow P_j'$, $\delta^* \leftarrow \frac{1}{(ts'+2)}$, $\rho_i^* \leftarrow (1-xi'/P_i')$, $\alpha_j^* \leftarrow (1-xj'/P_j')$, $\beta_i^* \leftarrow (1-xi'/P_i')$, $\omega_j^* \leftarrow (1-xi'/P_j')$, $\upsilon^* \leftarrow (1-x_{CH_2}'/P_{CH_2}')$, $\varphi^* \leftarrow (1-x_{CH_2}'/P_{CH_2}')$ $q^* = \frac{r_{CH_1}'+r_{CH_2}'}{(N_1 \times P^{S'}{}_i/\zeta + N_2 \times P^{S'}{}_j/\zeta + P^{S'}{}_{CH_2}/\zeta + P^{S'}{}_{CH_1}/\zeta + P_{ctx} + ts'P_{crx})}$; Flag =1and exit
else $q \leftarrow \frac{r_{CH_1}'+r_{CH_2}'}{(N_1 \times P^{S'}{}_i/\zeta + N_2 \times P^{S'}{}_j/\zeta + P^{S'}{}_{CH_2}/\zeta + P^{S'}{}_{CH_1}/\zeta + P_{ctx} + ts'P_{crx})}$, I=I+1, Flag =0
end if
until Flag=1 or I=I_{max}

iteration is Imax, then according to,[41] the computational complexity of ARCH algorithm is O(I_{max}Nlog(w)) where I_{max} is the number of iterations, w is the number of constraints in optimization problem, and N is the number of nodes in cluster. After solving OPT1, we can observe:

Lemma 2: ARCH converges to maximum $\mathcal{R}^{(\mathcal{P},\S,ts)}$ in each iteration.

Proof:

We have applied the Dinkelbach method as in to prove that $\bar{\mathcal{D}}(q)$ is strictly monotonically decreasing w.r.t q, where $\bar{\mathcal{D}}(.)$is the maximum of $\mathcal{D}(\mathcal{P}, \S, ts)$ with a given q. Also, $\bar{\mathcal{D}}(q) \geq 0$ for any value of q. Finally, q is increasing in each iteration. Hence, $\bar{\mathcal{D}}(q)$will converge to zero and will satisfy optimality of Lemma 1after enough iterations.

4.3 The proposed cluster head selection algorithm

In this section, we propose an algorithm for cluster head selection. The proposed algorithm is based on the values of the energy dissipated, explained in Section III. The algorithm starts by applying the conventional k-mean method. Then, for each cluster, the algorithm finds the best node that provides the best energy efficiency. Afterwards, the algorithm checks if the selected node has changed, then it repeats finding the best node that gives best energy efficiency until the node is not changed. This node will be the cluster head. Then, the algorithm will cluster the nodes among these cluster heads. Table 2 explains the pseudo code of the algorithm. The computational complexity of this algorithm is given by $O(N^2)$ because it is based on k-means algorithm, which has a time complexity of $O(N^2)$ where N is the input data size,[38]

Table 2. Cluster head selection algorithm.

1. Apply k-mean algorithm to cluster the network
2. Initialize CHs t, tϵ{1,2,,…,k}, N_k number of nodes in cluster k, N number of nodes in network, A={} is set of cluster heads that are one-hop away from HAP; B={} is set of cluster heads that are two-hop away from HAP.
3. For *t*=1 to *k*
4. Repeat
5. For *i*=1 to N_t
6. Find energy efficiency of i by applying Eq. (41), F_i
7. $t_{new} \leftarrow arg\ \max_i F_i$
8. end for
9. if $t \neq t_{new}$ then *remove t from , Update* N_t
10. until *t is no longer changed*
11. End if
12. If t is one-hop away from HAP then add t to A countA++ else add t to B countB++
13. End if
14. End for
15. Find achievable rate of cluster head t, R_t by Eq. (5)
16. // finding the best cluster head to join; // clustering the nodes among the cluster heads; N=N\{countA}
17. For j=1 to N
18. For a=1 to countA // for all cluster heads inside one-hop cluster A
19. Add j to cluster head a having $\max_a R_{ja}^S$
20. Remove j from N, Update N
21. End for
22. End for
23. // Same procedure for cluster heads that are two-hop away from HAP
24. // finding the best cluster head to join; // clustering the nodes among the cluster heads; N=N\{countB}
25. For j=1 to N
26. For a=1 to countB // for all cluster heads inside two-hop cluster B
27. Add j to cluster head a having $\max_a R_{ja}^S$
28. Remove j from N, Update N
29. End for
30. End for

4.4 Limitation of the proposed ARCH Scheme

The proposed ARCH scheme leverages the benefit of SWIPT technique aiming at enhancing the energy efficiency of cluster-based EHWSNs especially for the cooperative transmission between clusters. Since sensor nodes are subject to interference, ARCH scheme avoids having interference by applying scheduling mechanism where each node splits its associated timeslot for information transfer and energy harvesting. However, in the presence of HAP failure, the sensor nodes will not have any source of energy harvesting and this causes quick energy depletion. Hence, the authors suggested for future work a resilience-based system by applying prediction mechanism such as deep learning neural network for future prediction of node failure.

5. Performance evaluation

In this section, we evaluate the effectiveness of our proposed ARCH algorithm using MATLAB2019b. Table 3 summarizes the parameters used for simulation. We consider a simple distance-dependent path loss model given by $hi = Gd_i^{-\gamma}$ and $g_{ij} = Gd_{ij}^{-\gamma}$ assuming the channel fading effect to be averaged out over the frame and all of the channels to be reciprocal,[20,42] where G refers to the average power attenuation at a reference distance of 1 m and is set to -30 dB, and g is the path loss exponent, which is set to 2.5.[43] Here, d_i is the distance between HAP and any sensor node, i, d_{ij} is the distance between nodes i and j. For performance analysis, we compared ARCH with Choi and Lee,[17] Lu *et al.*,[31] and Shi *et al.*[21] in terms of energy efficiency, average achievable rate, and total energy dispelled.

Table 3. Simulation parameters.[21,17]

Parameter	Value
Field area	100x100 m2
Sensor nodes	[100, 200, 300, 400, 500]
Number of clusters, k	[8,16,24,32,36]
Transmission power of HAP, P	46dBm
Channel power gain, h_i	$Gd_i^{-\gamma}$
Energy efficiency, ζ	0.8
Energy ratio for transmission of sensor nodes, η	0.9
Energy ratio for transmission of CHs, η	0.7
Power attenuation at a reference distance 1m, G	-30dBm
Path loss exponent, γ	2.5
Constant circuit power consumption at transmitter, P_{ctx}	10dBm
Constant circuit power consumption at receiver, P_{crx}	10dBm
Maximum transmit power P_{max}	30dBm
Minimum required rate, R_{min}	30kbps
WPT slot, Te	5s
Time, T	10s
σ^2	-40,-50,-60dBm
Power amplifier efficiency ε	0.35
Number of simulation trials	1000

5.1 Energy efficiency analysis

This section illustrates the convergence of the proposed ARCH algorithm with different noise power values. Also, a comparison is carried out against different state-of-the-art algorithms. The simulations are carried out for N=300 and k=24.

In Fig. 4, we can see that the proposed ARCH algorithm converges after 4 iterations with highest energy efficiency value at noise power of -60dbm. This is because with high noise power the achievable rate is smaller and the power is larger than that of low noise power, which leads to low energy efficiency and vice versa.

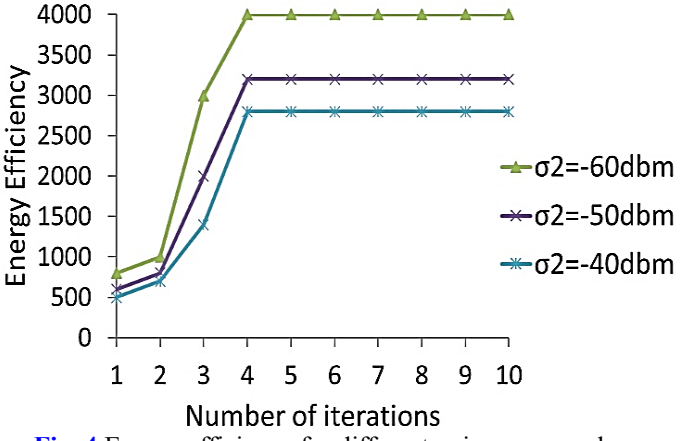

Fig. 4 Energy efficiency for different noise power values.

In order to verify the effectiveness of our proposed algorithm, we compared it with other state-of-the-art algorithms under same constraints with noise power of -40dbm. Fig. 5 shows the energy efficiency analysis for the proposed ARCH algorithm against Choi and Lee,[17] Lu *et al.*,[31] and Shi *et al.*.[21] As it can be seen, ARCH algorithm converges and achieves the highest energy efficiency value within 4 iterations. However, the energy efficiency for the rest of algorithms converges at the 5th iteration with lowest value for Choi and Lee, and highest value for Lu *et.al*. The first reason is because the benchmark schemes either apply the TS mode or the PS mode in their SWIPT algorithm without taking into consideration the dissipated energy; whereas the proposed ARCH scheme adapts the system conditions related to achievable data rates and system consumption power to apply the TS mode and PS mode. The second reason is because the proposed ARCH scheme applies the SWIPT technique for intra-cluster communications and inter-cluster communications which makes the cooperative transmission more effective.

Figure 6 shows the energy efficiency versus *Pmax* for different algorithms. As *Pmax* gradually increases from a small value, the energy efficiency increases rapidly until *Pmax* reaches 20dBm. This is because once the maximum efficiency

is achieved, an increase in transmit power will result in a decrease in energy efficiency. This is illustrated by Choi and Lee algorithm that maximizes only the throughput. Lu *et al*. and Shi *et al*. proposed schemes focus on achieving energy efficiency under various powers; yet both schemes didn't include the dissipated energy when considering the TS mode or PS mode. This demonstrates the importance of considering the energy efficiency in the proposed ARCH scheme. The proposed ARCH algorithm achieves the maximum energy efficiency among other algorithms.

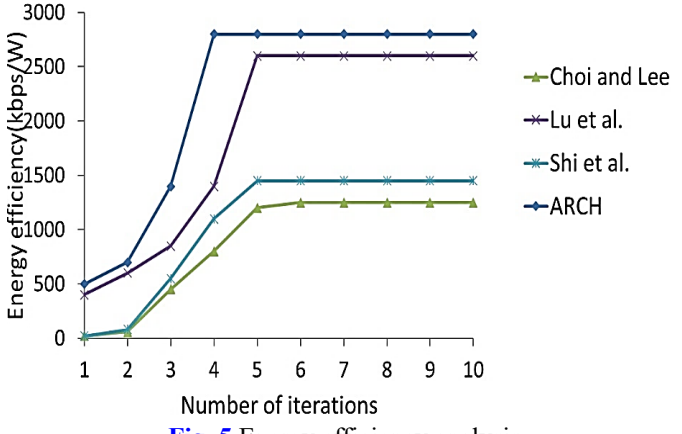

Fig. 5 Energy efficiency analysis.

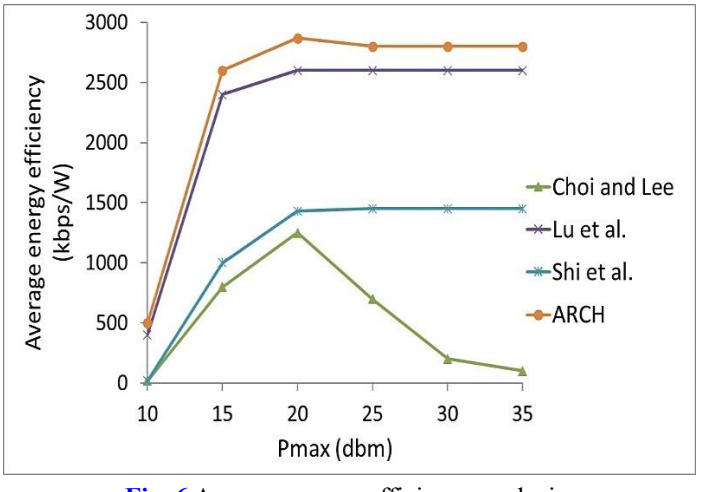

Fig. 6 Average energy efficiency analysis.

5.2 Average achievable rate analysis

Figure 7 shows the average achievable rate in a cluster versus number of sensor nodes for the proposed ARCH algorithm with k =24, in comparison with state-of-the-art algorithms. As it can be seen, when the number of sensor nodes increases in each cluster, the average achievable rate for the proposed ARCH increases. This is because the minimum achievable rate in a cluster increases significantly with the increase of sensor nodes. Once the number of sensor nodes increases, the total energy transferred to the cluster head increases and hence the total data rate increases. However, in the work of benchmark schemes, the minimum achievable rate in a cluster doesn't increase significantly with the increase of sensor nodes since the cluster heads depend only on the energy harvested from the HAP for intra-cluster communication and didn't consider transferring the energy between cluster heads for inter-cluster communication. This is illustrated in Fig. 7. Also, the benchmark schemes consider fixed CHs; however, the proposed ARCH algorithm takes into consideration the node that provides the best energy efficiency and accordingly nodes are clustered. This outperforms the ARCH scheme over other schemes.

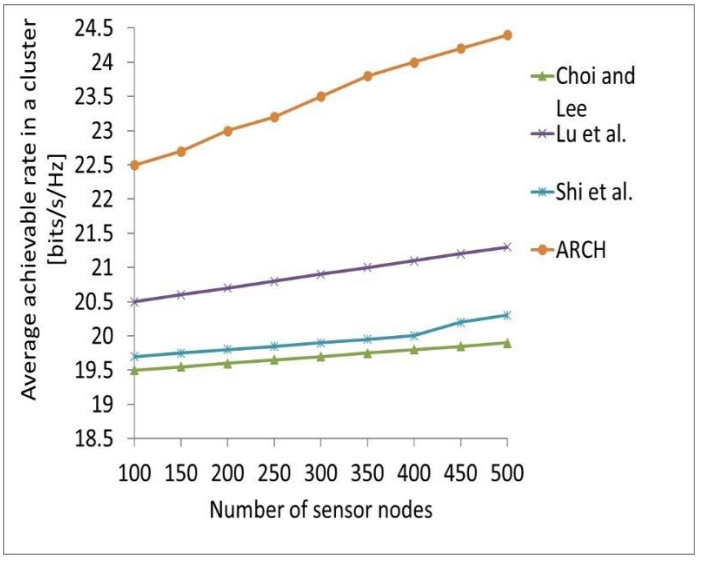

Fig. 7 Average achievable rate analysis.

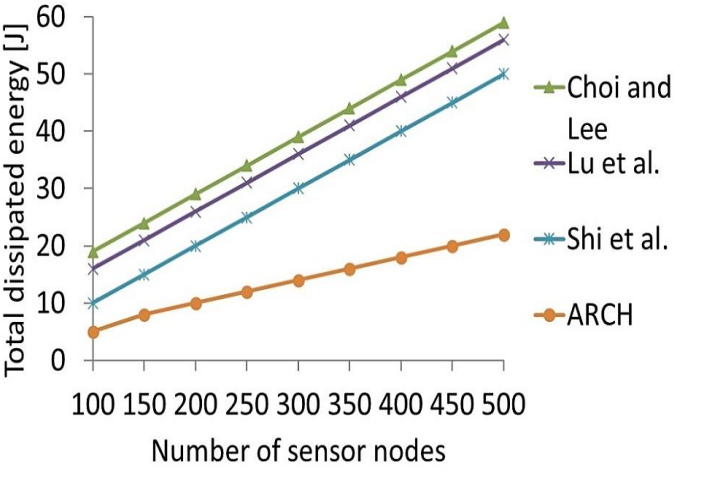

Fig. 8 Total dissipated energy analysis.

5.3 Total dissipated energy in network

Figure 8 shows the total energy dissipated in a network versus number of sensor nodes of k=24 for the proposed ARCH algorithm in comparison with other algorithms. As it can be seen, when the number of sensor nodes increases the total dissipated energy increases since the dissipated energy is linearly proportional to the number of sensor nodes. Also, the cluster head selection algorithm proves its positive impact on the total dissipated energy of the network since in the cluster head selection, the cluster dissipated energy is considered.

This technique doesn't exist in other benchmark algorithms. On the other hand, for the same number of sensor nodes (N=300) as the number of clusters, k increases, the dissipated energy in the network decreases since the number of nodes decreases in each cluster and so the achievable rate. This is illustrated in Fig. 8 and Fig. 9. The proposed ARCH algorithm shows the lowest dissipated energy compared to other benchmark schemes since ARCH scheme focuses on minimizing the wastage energy by harvesting energy consistent with the achievable data rate and allowing energy transfer for cooperative transfer between clusters. This explains why the proposed ARCH scheme outperforms other benchmark schemes.

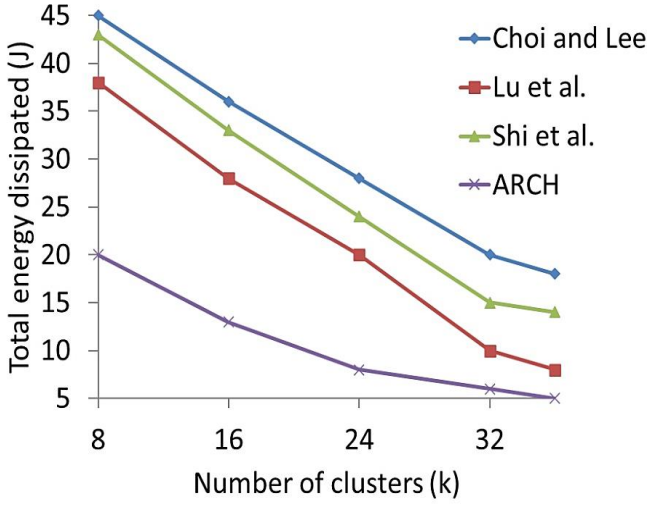

Fig. 9 Total dissipated energy versus number of clusters.

Fig. 10 Total energy dissipated comparison with and without SWIPT.

In Fig. 10, the total energy dissipated in each cluster is considered. We considered to have 8 clusters in the system. Same phenomena will be applied for 16, 24, and 32 clusters. Here, the effectiveness of the proposed clustering algorithm which is based on SWIPT is revealed. Therefore, we compared the proposed SWIPT-based clustering algorithm to clustering algorithm without the use of SWIPT. It can be seen that the energy dissipated when SWIPT is used is lesser than of non-SWIPT clustering algorithm. This is because, in each cluster, each node transfers its remaining energy to the CH through SWIPT and the CH uses it to transmit its data. Since the rate of the CHs in Cluster 3 and Cluster 5 is higher than the rate of the cluster members (*i.e.*, $R_i > \min_j R_{ji}$), so Clusters 3 and 5 have a dissipated energy distribution similar to that in the non-SWIPT scheme. All in all, the energy dissipated for the proposed SWIPT-based clustering algorithm is approximately 70% better than that of the non-SWIPT-based clustering algorithm.

6. Conclusion

In this paper, optimizing the resource allocation for hybrid SWIPT-based WPSNs was studied. Based on the node's dispersed power level, the node adaptively chooses between the PS mode and TS mode for communication. We formulated the resource allocation maximization problem as a non-convex optimization problem by jointly optimizing the SWIPT ratios for both PS and TS modes, transmit powers, achievable rates, and the time for transmission for intra-cluster communication and inter-cluster communication. We have proposed ARCH algorithm which is Dinkelbach-based iterative method to obtain the optimal solution for the EE maximization problem. Also, we proposed a cluster head selection algorithm that considers the energy efficiency value for the cluster head selection. The effectiveness of the proposed SWIPT-based clustering algorithm is revealed by analysing the energy dissipated in each cluster when compared with non-SWIPT clustering algorithm. In fact, this is the first time to consider an adaptive selection of SWIPT mode for a cooperative transmission in a hybrid SWIPT-enabled wireless powered sensor networks. Simulations show the superiority of ARCH over other state-of-the-art algorithms in terms of energy efficiency, achievable rate, and dissipated energy. As for future work, we will extend our work by releasing the assumption of having one-hop and two-hops cluster heads to include m-hops cluster heads away from the HAP for large sensor networks. Furthermore, we are interested in exploring the relationship between the number of nodes in a cluster and the duration of the time slots for different environmental and channel conditions as well as enhancing the resilience of the proposed scheme by applying prediction mechanism such as deep learning neural network.

Conflict of Interest

There is no conflict of interest.

Supporting Information

Not applicable.

Appendix

Transforming OPT 4= $\max_{(P,ş,ts)}$ Đ(P, ş,ts) into a convex optimization problem:

Since the objective function of OPT4 is a linear function with respect to şr and Pr rϵ $N_1 \cup N'_2$; and C1 - 2; C2 - 2; C3-1; C5 - 1;C4,C6-C11, are linear constraints, whether OPT4 is convex or doesn't depend on constraints C12 and C13. That is, if both functions $f1(Pi; xi) = \log_2\left(1 + \frac{(Pi-xi)|h_i|^2}{\sigma^2}\right)$ and $f2(ts; P_{CH1}) = ts \log_2\left(1 + \frac{(PCH1)|h_{CH1}|^2}{\sigma^2}\right)$, are concave, then OPT4 is convex. Let $Vr = \frac{|hi|^2}{\sigma^2}$ Taking the second order derivative of $f_1(Pr; xr)$, the Hessian matrix is given by:

$$\frac{\partial^2 f1(Pr;\, xr)}{\partial (Pr;\, xr)^2} = \begin{bmatrix} \frac{-Vr^2}{(1+(Pi-xi))^2 \ln 2} & \frac{Vr^2}{(1+(Pi-xi))^2 \ln 2} \\ \frac{Vr^2}{(1+(Pi-xi))^2 \ln 2} & \frac{-Vr^2}{(1+(Pi-xi))^2 \ln 2} \end{bmatrix} \leq 0;\ i\epsilon\, \mathcal{N}$$

Thus, $f_1(Pi; xi)$ is concave. Same procedure is done for $f_2(ts; P_{CH1})$. Therefore, the optimization problem OPT4 is convex.

References

[1] Q. Wang, H.-N. Dai, Z. Zheng, M. Imran, A. Vasilakos, On connectivity of wireless sensor networks with directional antennas, *Sensors*, 2017, **17**, 134, doi: 10.3390/s17010134.

[2] Y. Zhang, H. Gao, S. Cheng, J. Li, An efficient EH-WSN energy management mechanism, *Tsinghua Science and Technology*, 2018, **23**, 406-418, doi: 10.26599/TST.2018.9010034.

[3] L. P. Qian, G. Feng, V. C. M. Leung, Optimal transmission policies for relay communication networks with ambient energy harvesting relays, *IEEE Journal on Selected Areas in Communications*, 2016, **34**, 3754-3768, doi: 10.1109/JSAC.2016.2621356.

[4] H. Sharma, A. Haque, Z. A. Jaffery, Maximization of wireless sensor network lifetime using solar energy harvesting for smart agriculture monitoring, *Ad Hoc Networks*, 2019, **94**, 101966, doi: 10.1016/j.adhoc.2019.101966.

[5] Y. K. Tan, S. K. Panda, Optimized wind energy harvesting system using resistance emulator and active rectifier for wireless sensor nodes, *IEEE Transactions on Power Electronics*, 2011, **26**, 38-50, doi: 10.1109/TPEL.2010.2056700.

[6] Y. Huang, B. Clerckx, Waveform design for wireless power transfer with limited feedback, *IEEE Transactions on Wireless Communications*, 2018, **17**, 415-429, doi: 10.1109/twc.2017.2767578.

[7] T. Liu, X. Qu, F. Yin, Y. Chen, Energy efficiency maximization for wirelessly powered sensor networks with energy beamforming, *IEEE Communications Letters*, 2019, **23**, 2311-2315, doi: 10.1109/LCOMM.2019.2942920.

[8] M. Song, M. Zheng, Energy efficiency optimization for wireless powered sensor networks with nonorthogonal multiple access, *IEEE Sensors Letters*, 2018, **2**, 1-4, doi: 10.1109/LSENS.2018.2792454.

[9] L. Sun, L. Wan, K. Liu, X. Wang, Cooperative-evolution-based WPT resource allocation for large-scale cognitive industrial IoT, *IEEE Transactions on Industrial Informatics*, 2020, **16**, 5401-5411, doi: 10.1109/TII.2019.2961659.

[10] W. Yang, W. Mou, X. Xu, W. Yang, Y. Cai, Energy efficiency analysis and enhancement for secure transmission in SWIPT systems exploiting full duplex techniques, *IET Communications*, 2016, **10**, 1712-1720, doi: 10.1049/iet-com.2015.1147.

[11] Y. Huang, M. Liu, Y. Liu, Energy-efficient SWIPT in IoT distributed antenna systems, *IEEE Internet of Things Journal*, 2018, **5**, 2646-2656, doi: 10.1109/JIOT.2018.2796124.

[12] D. W. K. Ng, E. S. Lo, R. Schober, Energy-efficient resource allocation for secure OFDMA systems, *IEEE Transactions on Vehicular Technology*, 2012, **61**, 2572-2585, doi: 10.1109/TVT.2012.2199145.

[13] H.-H. Choi, J.-R. Lee, Energy-neutral operation based on simultaneous wireless information and power transfer for wireless powered sensor networks, *Energies*, 2019, **12**, 3823, doi: 10.3390/en12203823.

[14] B. Krishnamachari, D. Estrin, S. Wicker, Modelling data-centric routing in wireless sensor networks, *IEEE Infocom*, 2002, **2**, 39-44.

[15] H.-H. Choi, Construction of energy-efficient data aggregation tree in wireless sensor networks, *The Journal of Korean Institute of Communications and Information Sciences*, 2016, **41**, 1057-1059, doi: 10.7840/kics.2016.41.9.1057.

[16] L. Liu, R. Zhang, K.-C. Chua, Multi-antenna wireless powered communication with energy beamforming, *IEEE Transactions on Communications*, 2014, **62**, 4349-4361, doi: 10.1109/TCOMM.2014.2370035.

[17] L. Shi, Y. Ye, R. Q. Hu, H. Zhang, Energy efficiency maximization for SWIPT enabled two-way DF relaying, *IEEE Signal Processing Letters*, 2019, **26**, 755-759, doi: 10.1109/LSP.2019.2906463.

[18] X. Liu, X. B. Zhai, W. Lu, C. Wu, QoS-guarantee resource allocation for multibeam satellite industrial Internet of Things with NOMA, *IEEE Transactions on Industrial Informatics*, 2021, **17**, 2052-2061, doi: 10.1109/TII.2019.2951728.

[19] Y. Huang, B. Clerckx, Waveform design for wireless power transfer with limited feedback, *IEEE Transactions on Wireless Communications*, 2018, **17**, 415-429, doi: 10.1109/TWC.2017.2767578.

[20] L. Sun, L. Wan, K. Liu, X. Wang, Cooperative-evolution-based WPT resource allocation for large-scale cognitive industrial IoT, *IEEE Transactions on Industrial Informatics*, 2020, **16**, 5401-5411, doi: 10.1109/TII.2019.2961659.

[21] W. Yang, W. Mou, X. Xu, W. Yang, Y. Cai, Energy efficiency analysis and enhancement for secure transmission in SWIPT systems exploiting full duplex techniques, *IET Communications*, 2016, **10**, 1712-1720, doi: 10.1049/iet-com.2015.1147.

[22] J. Tang, D. K. C. So, A. Shojaeifard, K.-K. Wong, J. Wen, Joint antenna selection and spatial switching for energy efficient MIMO SWIPT system, *IEEE Transactions on Wireless Communications*, 2017, **16**, 4754-4769, doi: 10.1109/TWC.2017.2702575.

[23] H. Dai, Y. Huang, C. Li, S. Li, L. Yang, Energy-efficient resource allocation for device-to-device communication with

WPT, IET Communications, 2017, **11**, 326-334, doi: 10.1049/iet-com.2015.1192.
[24] J. Tang, D. K. C. So, A. Shojaeifard, K.-K. Wong, J. Wen, Joint antenna selection and spatial switching for energy efficient MIMO SWIPT system, IEEE Transactions on Wireless Communications, 2017, **16**, 4754-4769, doi: 10.1109/TWC.2017.2702575.
[25] D. K. P. Asiedu, S.-J. Shin, K. Koumadi, K.-J. Lee, Review of simultaneous wireless information and power transfer in wireless sensor networks, *Journal of Information and Communication Convergence Engineering*, 2019, **17**, 105-116, doi: 10.6109/jicce.2019.17.2.105.
[26] M. A. Hossain, R. Md Noor, K.-L. Alvin Yau, I. Ahmedy, S. S. Anjum, A survey on simultaneous wireless information and power transfer with cooperative relay and future challenges, *IEEE Access*, 2019, **7**, 19166-19198, doi: 10.1109/ACCESS.2019.2895645.
[27] T. D. Ponnimbaduge Perera, D. N. K. Jayakody, S. K. Sharma, S. Chatzinotas, J. Li, Simultaneous wireless information and power transfer (SWIPT): recent advances and future challenges, *IEEE Communications Surveys & Tutorials*, 2018, **20**, 264-302, doi: 10.1109/comst.2017.2783901.
[28] T. Liu, X. Wang, L. Zheng, A cooperative SWIPT scheme for wirelessly powered sensor networks, *IEEE Transactions on Communications*, 2017, **65**, 2740-2752, doi: 10.1109/TCOMM.2017.2685580.
[29] B. Tong, Z. Li, G. Wang, W. Zhang, How wireless power charging technology affects sensor network deployment and routing. 2010 IEEE 30th International Conference on Distributed Computing Systems. June 21-25, 2010, Genoa, Italy. IEEE, 2010, 438-447, doi: 10.1109/ICDCS.2010.61.
[30] L. Shi, J. Han, D. Han, X. Ding, Z. Wei, The dynamic routing algorithm for renewable wireless sensor networks with wireless power transfer, *Computer Networks*, 2014, **74**, 34-52, doi: 10.1016/j.comnet.2014.08.020.
[31] H. Han, X.-m. Liu, H.-y. Huang, F. Wan, Energy efficient routing for multi-hop clustered energy efficient routing for multi-hop clustered, ResearchSquare, 2020, **1**, 2-24, doi: 10.3390/s21020627.
[32] H. Ju, R. Zhang, Throughput maximization in wireless powered communication networks, *IEEE Transactions on Wireless Communications*, 2014, **13**, 418-428, doi: 10.1109/TWC.2013.112513.130760.
[33] M. R. U. Rehman, I. Ali, D. Khan, M. Asif, P. Kumar, S. J. Oh, Y. G. Pu, S.-S. Yoo, K. C. Hwang, Y. Yang, D. I. Kim, K.-Y. Lee, A design of adaptive control and communication protocol for SWIPT system in 180 nm CMOS process for sensor applications, *Sensors*, 2021, **21**, 848, doi: 10.3390/s21030848.
[34] B. Krishnamachari, D. Estrin, S. Wicker, Modeling data-centric routing in wireless sensor networks, *IEEE Infocom*, New York, NY, USA, 2002.
[35] H.-H. Choi, Construction of energy-efficient data aggregation tree in wireless sensor networks, *The Journal of Korean Institute of Communications and Information Sciences*, 2016, **41**, 1057-1059, doi: 10.7840/kics.2016.41.9.1057.
[36] S. K. Singh, P. Kumar, J. P. Singh, A survey on successors of LEACH protocol, *IEEE Access*, 2017, **5**, 4298-4328, doi: 10.1109/access.2017.2666082.
[37] D. W. K. Ng, E. S. Lo, R. Schober, Energy-efficient resource allocation in multi-cell OFDMA systems with limited backhaul capacity, *IEEE Transactions on Wireless Communications*, 2012, **11**, 3618-3631, doi: 10.1109/TWC.2012.083112.111951.
[38] W. Dinkelbach, On nonlinear fractional programming, *Management Science*, 1967, **13**, 492-498, doi: 10.1287/mnsc.13.7.492.
[39] S. Boyd, L. Vandenberghe, Convex Optimization. Cambridge: Cambridge University Press, 2004, doi: 10.1017/cbo9780511804441
[40] X. Kang, C. K. Ho, S. Sun, Full-duplex wireless-powered communication network with energy causality, *IEEE Transactions on Wireless Communications*, 2015, **14**, 5539-5551, doi: 10.1109/TWC.2015.2439673.
[41] H.-H. Choi, W. Shin, Slotted ALOHA for wireless powered communication networks, *IEEE Access*, 2018, **6**, 53342-53355, doi: 10.1109/access.2018.2871068.
[42] W. Lu, X. Xu, G. Huang, B. Li, Y. Wu, N. Zhao, F. R. Yu, Energy efficiency optimization in SWIPT enabled WSNs for smart agriculture, *IEEE Transactions on Industrial Informatics*, 2021, **17**, 4335-4344, doi: 10.1109/TII.2020.2996672.
[43] D. W. K. Ng, E. S. Lo, R. Schober, Wireless information and power transfer: energy efficiency optimization in OFDMA systems, *IEEE Transactions on Wireless Communications*, 2013, **12**, 6352-6370, doi: 10.1109/TWC.2013.103113.130470.